Proceedings of the ASME 27th International Conference on Offshore Mechanics and Arctic Engineering
OMAE2008
June 15-20, 2008, Estoril, Portugal

OMAE2008-57481

A GENERIC METHOD TO MODEL FREQUENCY-DIRECTION WAVE SPECTRA FOR FPSO MOTIONS

Hermione J. van Zutphen
Shell International Exploration and Production
Rijswijk ZH, The Netherlands
Hermione.vanZutphen@SHELL.com

Philip Jonathan
Shell Global Solutions
Shell Technology Centre Thornton, Chester UK

Kevin C. Ewans
Shell International Exploration and Production
Rijswijk ZH, The Netherlands

ABSTRACT

We report a new approach to model the frequency-direction spectrum, in which the frequency-direction spectra from measurements or hindcast studies are fitted simultaneously in two dimensions, frequency and direction. Depending on the amount of wind forcing on the partition, either a unimodal (swell) or bimodal (wind-sea) wave spreading function is adopted together with the spectral form which best fits the frequency spectrum. This paper describes the new method and presents the results on a measured dataset.

Key words: frequency-direction spectra, waves, wave spreading, vessel motions

INTRODUCTION

Waves are an important driver in the design of offshore structures and floating systems. A better understanding of the wave climate reduces the uncertainties in the design of offshore systems. A recent development in directional wave spectral analysis is the software package XWaves for spectral partitioning. Based on an approach, originally developed by the Applied Physics Lab of John Hopkins University (Hanson & Phillips, 2001), the software extracts the wind-sea and swell components in the wave spectrum and the amount of wind forcing on each component, for large datasets. Additionally, it tracks the development of the swell systems, which can be generated by storms thousands of kilometres away.

Presently, the resulting 2D frequency-direction components of the spectrum (partitions) are reduced to frequency spectra and fitted to a particular spectral form, such as a JONSWAP spectrum. The resulting parameters are then used in long term response analyses of vessel motions. While the mean direction of each component is retained, general forms for the directional spreading functions are used; the specific directional spreading details are therefore lost. Previous studies (for example, HSE 2002) have shown that (turret) moored vessels respond differently to short crested seas than to long crested seas, and therefore, adding directional information directly from the wave spectrum to the parametrized spectrum should improve the accuracy of the calculated responses.

Studies from for example Ewans, 1998 and Hwang et al, 2000, have shown that wind seas are bimodal at frequencies greater than the peak frequency, while swell components have been shown to be unimodal (Ewans, 2002). In fitting the spectra to directional distribution models for both wind-sea and swell, the bi-modality for wind-seas is retained.

NOMENCLATURE

$S_i(f,\theta)$	frequency-direction spectrum
$A_i(f,\theta)$	spreading function
f	frequency (range)
f_p	peak frequency
θ	direction (range)

$\Delta\theta$	angular separation $\theta_H - \theta_L$ of the direction peaks
α, β, γ	fitting parameters for σ and $\Delta\theta$
ε	error term

LOCATION OF FREQUENCY-DIRECTION SPECTRA

For the validation of the model, observations of frequency-direction spectra made near the site of the Maui-A platform off the West Coast of New Zealand are used.

Parameter values for the fits obtained during studies to derive directional distributions for wind-seas (Ewans, 1998) and swell (Ewans, 2002) are used in this study as starting guess for the fitting procedure. The Maui location has been proven to produce well-defined fetch-limited seas due to south-east winds (Ewans and Kibblewhite, 1990) which conform closely to the JONSWAP spectrum. Also, at this location, a more or less constant swell component originating from the Southern Ocean is observed.

THEORETICAL BACKGROUND

The 2-dimensional frequency-direction spectrum $S(f,\theta)$ of a sea state can be described as the sum of its wind sea (index *0)* and *1 to n* swell partitions:

$$S(f,\theta) = \sum_{i=1}^{n} S_i(f)\, A_i(f,\theta) + S_0(f)\, A_0(f,\theta) \tag{1.1}$$

where $S_i(f)$ denotes the frequency spectrum for partition *i* and $A_i(f,\theta)$ the spreading function which yields:

$$\int_{-\pi}^{\pi} A_i(f,\theta)\, d\theta = 1 \tag{1.2}$$

While in case of buoy measurements, the directional spreading function can be estimated using either a model-independent estimate (like the maximum entropy method (MEM) or the maximum likelihood method (MLM)) from the Fourier coefficients, in this case, we need a parametric description of the directional spreading function.

Wind seas have been shown by for example Ewans, 1998 and Hwang et al., 2000 to be bimodal at frequencies larger than the peak frequency. Ewans (1998) proposed a double-peaked form for the directional distribution, based on a double Gaussian functions defined as:

$$A_0(f,\theta) = \frac{1}{\sqrt{8\pi}\,\sigma_0(f)} \sum_{k=-\infty}^{\infty} \left\{ \exp\left(-\frac{\left(\theta - \theta_L(f) - 2\pi k\right)^2}{2\sigma_0^2(f)} \right) + \exp\left(-\frac{\left(\theta - \theta_H(f) - 2\pi k\right)^2}{2\sigma_0^2(f)} \right) \right\} \tag{1.3}$$

where σ_0 is the angular width and a measure for the spreading of each component (circular rms spreading) and θ_L and θ_H are the locations of the peaks centered at equal angles on each side of the mean wave direction. The circular rms spreading σ_0 can be parametrized using the following form:

$$\sigma_0 = \begin{cases} \alpha_1 + \alpha_2 \left(\dfrac{f}{f_{p0}} \right)^{\alpha_4} & \text{for } f < f_{p0} \\ \alpha_{temp} + \alpha_3 \left(\dfrac{f}{f_{p0}} \right)^{\alpha_5} & \text{for } f \geq f_{p0} \end{cases} \tag{1.4}$$

Ewans (1998) proposed the following values for the rms spreading for wind-seas:

$$\begin{aligned} \alpha_1 &= 11.38 \\ \alpha_2 &= 5.357 \\ \alpha_3 &= -15.39 \\ \alpha_4 &= -7.929 \\ \alpha_5 &= -2 \\ \alpha_{temp} &= 32.13 \end{aligned} \tag{1.5}$$

The location of the peaks of the spectrum is given by:

$$\begin{aligned} \theta_H(f) &= \bar{\theta}(f) + \frac{\Delta\theta(f)}{2} \\ \theta_L(f) &= \bar{\theta}(f) - \frac{\Delta\theta(f)}{2} \end{aligned} \tag{1.6}$$

with $\Delta\theta$ the angular separation, $\theta_H - \theta_L$,of the peaks. The angular separation can be written in the form (Ewans, 1998):

$$\Delta\theta = \begin{cases} \beta_1 & \text{for } f < f_{p0} \\ \exp\left(\beta_{temp} - \beta_2 \dfrac{f}{f_{p0}} \right) & \text{for } f > f_{p0} \end{cases} \tag{1.7}$$

with

$$\begin{aligned}\beta_1 &= 14.93\\ \beta_2 &= 5.453\\ \beta_{temp} &= 2.750\end{aligned} \tag{1.8}$$

Ocean swell is less spread and less likely to have a bimodal directional distribution (Ewans, 2002), and therefore, the directional distribution function reduces to:

$$A_i(f,\theta) = \frac{1}{\sqrt{2\pi}\sigma_i(f)} \sum_{k=-\kappa}^{\kappa} \left\{ \exp\left(-\frac{\left(\theta - \theta_i(f) - 2\pi k\right)^2}{2\sigma_i^2(f)} \right) \right\} \quad \forall i = 1,2,...,n \tag{1.9}$$

where the circular rms spreading is parametrized using a similar form as (1.4):

$$\sigma_i = \begin{cases} \gamma_{1i} + \gamma_{2i}\left(\frac{f}{f_{pi}}\right)^{\gamma_{4i}} & \text{for } f < f_{p0} \\ \gamma_{temp} + \gamma_{3i}\left(\frac{f}{f_{pi}}\right)^{\gamma_{5i}} & \text{for } f \geq f_{p0} \end{cases} \tag{1.10}$$

with the following values obtained from Ewans' fit:

$$\begin{aligned}\gamma_1 &= 6\\ \gamma_2 &= 4\\ \gamma_3 &= 46\\ \gamma_4 &= -5\\ \gamma_5 &= 0.3\\ \gamma_{temp} &= -36\end{aligned} \tag{1.11}$$

for each component.

GENERALIZED PARAMETRIC DESCRIPTION OF FREQUENCY-DIRECTION SPECTRUM

The model can be generalized by assuming a common form for both wind-sea and swell components, by noting the fact that the directional distribution for swell components has the same form as a wind-sea component with a angular separation $\Delta\theta = 0$ (unimodal). This generalization will offer the advantage that the parameters can be modeled smoothly in time. The parametric description of the spreading distribution functions can then be generalized as follows:

$$S(f,\theta) = \sum_{i=1}^{n} S_i(f) N_i(f,\theta) \quad \forall i = 0,1,...n \tag{2.1}$$

with $i = 0$ indicating the wind-sea component and i > 0 for the swell components. $N_i(f,\theta)$ are the normalized 2D spectra which now take the common form:

$$N(f,\theta) = \frac{1}{\sqrt{8\pi}\sigma_0(f)} \sum_{k=-\kappa}^{\kappa} \left\{ \exp\left(-\frac{\left(\theta - \theta_{Li}(f) - 2\pi k\right)^2}{2\sigma_0^2(f)} \right) + \exp\left(-\frac{\left(\theta - \theta_{Hi}(f) - 2\pi k\right)^2}{2\sigma_0^2(f)} \right) \right\} \tag{2.2}$$

For swell components, $\theta_{Li} = \theta_{Hi}$ and (2.2) will reduce to (1.9). Using (1.4) and (1.10), the common form for the angular rms spreading can now be written as:

$$\sigma_i(f) = \begin{cases} \alpha_{1i} + \alpha_{2i}\left(\frac{f}{f_{pi}}\right)^{\alpha_{4i}} & \text{for } f < f_{pi} \\ \alpha_{tempi} + \alpha_{3i}\left(\frac{f}{f_{pi}}\right)^{\alpha_{5i}} & \text{for } f \geq f_{pi} \end{cases} \tag{2.3}$$

At $f = f_{p0}$ we have an equality constraint:

$\alpha_{1i} + \alpha_{2i} = \alpha_{tempi} + \alpha_{3i}$ which can be used to eliminate α_{tempi} to yield a single expression:

$$\sigma_i(f) = \alpha_{1i} + \alpha_{2i}\left(\left(1 - I_{f \geq f_{pi}}\right)\left(\frac{f}{f_{pi}}\right)^{\alpha_{4i}} + I_{f \geq f_{pi}} \right) + ... \alpha_{3i} I_{f \geq f_{pi}} \left(\left(\frac{f}{f_{pi}}\right)^{\alpha_{5i}} - 1 \right) \tag{2.4}$$

where I_x is an indicator function equal to 1 for $x \geq 0$ and 0 otherwise. Further, for the angular separation, we can now write:

$$\begin{aligned}\theta_{Hi}(f) &= \overline{\theta}_i(f) + \frac{\Delta\theta_i(f)}{2}\\ \theta_{Li}(f) &= \overline{\theta}_i(f) - \frac{\Delta\theta_i(f)}{2}\end{aligned} \tag{2.5}$$

and $\Delta\theta_i$ takes the form:

$$\Delta\theta_i(f) = \begin{cases} \beta_{1i} & \text{for } f < f_{pi} \\ \exp\left(\beta_{tempi} - \beta_{2i}\frac{f}{f_{pi}} \right) & \text{for } f > f_{pi} \end{cases} \tag{2.6}$$

At $f = f_{p0}$ we have an equality constraint:

$\beta_{1i} = \exp\left(\beta_{tempi} - \beta_{2i}\right)$ which can be used to eliminate β_{2i} to yield a single expression:

$$\Delta\theta_i(f) = \beta_{1i} \exp\left\{\beta_{2i}\left(1 - \left(\frac{f}{f_{pi}}\right)^{-1}\right)_+\right\} \qquad (2.7)$$

where $(x)_+ = 1$ if $x \geq 0$ and 0 otherwise.

The models can now be solved using a parameter fitting procedure, in this case a Maximum Likelihood Method. The frequency spectra are assumed to be known, with for example a JONSWAP or Gaussian spectrum. For each wave component $i = 0,1,...,n$, we need to fit the parameters of the generalized model for the frequency-direction spectra: $\{\alpha_{1i}, \alpha_{2i}, \alpha_{3i}, \alpha_{4i}, \alpha_{5i}, \beta_{1i}, \beta_{2i}\}$. However, the decrease the amount of work for the solver, the exponents $\{\alpha_{4i}, \alpha_{5i}\}$ can be set to fixed values like for example to values specified in the Maui directional distributions.

MAXIMUM LIKELIHOOD ESTIMATION

We assume that the measured spectra are taken from the model:

$$y_k = S_k + \varepsilon_k \qquad \varepsilon_k \sim N(0, \nu^2) \qquad (3.1)$$

where the index *k* refers to the grid of values $x_k = (f_i, \theta_j)$ with $(i = 1,2,...,m_1,\ j = 1,2,...,m_2, m = m_1 \times m_2)$ at which the spectral data is available. The error terms ε are identically and independently normally-distributed with constant variance ν^2.

The likelihood of the observed spectral data $\{y_k\}_{k=1}^n$ is given by:

$$L = \prod_{k=1}^{m} \frac{1}{\sqrt{2\pi}\nu} \exp\left(-\frac{\left(y_k - S(x_k;\lambda)\right)^2}{2\nu^2}\right) \qquad (3.2)$$

and the negative log-likelihood by:

$$l^* = \frac{m}{2}\log(2\pi) + m\log(\nu) + \sum_{k=1}^{m} \frac{\left(y_k - S(x_k;\lambda)\right)^2}{2\nu^2} \qquad (3.3)$$

Since m and ν are constants, this is effectively l:

$$l = \sum_{k=1}^{m} \left(y_k - S(x_k;\lambda)\right)^2 \qquad (3.4)$$

which is simply least squares. We note however that maximum likelihood provides a natural framework for incorporation of (e.g.) measurement error ν^2 which varies with frequency and direction.

Maximum likelihood estimates are obtained by setting the partial derivatives of l with respect to each component of α and β to zero and solving:

$$\frac{\partial l}{\partial \eta_i} = 0 \qquad \forall \eta_i \in \{\alpha_{1i}, \alpha_{2i}, \alpha_{3i}, \beta_{1i}, \beta_{2i}\}_{i=0}^n \qquad (3.5)$$

Since $S = S(x_k;\lambda)$, we can solve using the chain rule:

$$\frac{\partial l}{\partial \eta_i} = \sum_{j=0}^{n} \frac{\partial l}{\partial \lambda_j}\frac{\partial \lambda_j}{\partial \eta_i} \text{ where } \lambda_j \in \{\sigma_i, \Delta\theta\}_{i=0}^n \qquad (3.6)$$

In terms of S, we have:

$$\frac{\partial l}{\partial \eta_i} = \sum_{j=0}^{n}\left(\sum_{k=1}^{m} 2\left(S(x_k) - y_k\right)\frac{\partial S(x_k)}{\partial \lambda_j}\right)\frac{\partial \lambda_j}{\partial \eta_i} \qquad (3.7)$$

To solve, we need to evaluate the derivatives $\frac{\partial S(x_k)}{\partial \lambda_j}$ and $\frac{\partial \lambda_j}{\partial \eta_i}$ for all possible $\eta_i \in \{\alpha_{1i}, \alpha_{2i}, \alpha_{3i}, \beta_{1i}, \beta_{2i}\}_{i=0}^n$ and $\lambda_j \in \{\sigma_i, \Delta\theta_i\}_{i=0}^n$.

IMPLEMENTATION

The maximum likelihood equations are solved using MATLAB (with Optimization Toolbox). The fitting algorithm is initially fed with a starting guess, for which the spectrum is calculated. By perturbing the starting guess, the algorithm tries to find the minimum of the negative log-likelihood. The best guess of this first set of perturbations is then used to start a second set of perturbations. The number of perturbations is important to make sure that the algorithm is finding the solution at the lowest (global) minimum of the negative log-likelihood functions, instead of a local minimum, which will return a less optimal solution.

1. Establish quality of least squares fit at starting guess $g_o = \{\alpha_{1i}, \alpha_{2i}, \alpha_{3i}, \beta_{1i}, \beta_{2i}\}_{i=0}^n$
2. Uniform random perturbation g_o to find new starting guesses for the least squares problem. Optimization with smaller tolerance.
3. Iteration of step 2
4. Optimal solution is returned.

The algorithm was tested with model spectra obtained for the theoretical distributions from the Maui data for 3 cases (see Table 1):

- bimodal sea state consisting of pronounced wind sea and swell component.
- unimodal wind-sea with a very small swell component
- unimodal swell with a very small wind-sea component

Table 1 Significant wave height Hs and peak period Tp for the 3 theoretical model spectra.

Spectrum	Wind-sea		Swell	
	Hs (m)	Tp (s)	Hs (m)	Tp (s)
1	4	8.3	0.3	14.3
2	0.1	8.3	4	14.3
3	2.5	8.3	1	14.3

The model data is generated to conform to the parameter values given in (1.5) and (1.8) for wind-seas and (1.11) for swells. To test the convergence of the algorithm, both a good guess (the original parameters) and a bad guess are used to fit the data:

Table 2 Good and bad starting guesses used to test the method.

Wind-sea ($i=0$)	α_{1i}	α_{2i}	α_{3i}	β_{1i}	β_{2i}
Good	11.4	5.4	-15.4	14.9	2.8
Bad	15	3	-18	12	4
Swell ($i>0$)					
Good	6	4	46	0	0
Bad	2	2	55	0	0

The value for α_{4i} is fixed –7.9 for wind sea and –5 for swell components, and α_{5i} is fixed to respectively –2 and 0.3.

Figures 1,2 and 3 give the resulting log-spectra of the model spectra. In Table 3 the mean, standard deviation and the RMS error of the starting guess and the optimum fit are given relative to the true spectrum. The fitting algorithm is well able to fit the energy peaks and the right variation in the spectrum. The goodness of fit results show that the fitting procedure has significantly improved the starting guess of the spectrum and that both the mean value and the standard deviation are retained in the resulting optimum.
However, the tail of specifically the wind-sea component is much wider spread than the true spectrum and when the energy content of the wind-sea is low, the bimodality seems to disappear. A possible improvement to the method would be to preferentially penalise poor fitting of spectral tails by introducing non-constant ν^2, or alternatively to reformulate the maximum likelihood form to fit to the log-spectrum instead of the normal spectrum.

Table 3 Goodness of fit results for the optimum fits for the 3 theoretical model spectra with a bad starting guess.

Spectrum 1	Mean	Std	RMS error
True spectrum	0.005605	0.028395	
Starting guess	0.005607	0.028108	1.79e-006
Optimum Fit	0.005605	0.028377	9.93e-011

Spectrum 2	Mean	Std	RMS error
True spectrum	0.005615	0.062155	
Starting guess	0.005867	0.106212	2.52e-004
Optimum Fit	0.005615	0.061921	4.98e-010

Spectrum 3	Mean	Std	RMS error
True spectrum	0.002528	0.011694	
Starting guess	0.002544	0.012783	1.56e-005
Optimum Fit	0.002528	0.011686	7.56e-011

APPLICATION TO MAUI DATA

Additionally, the fitting method has been applied to observed wave spectra a Maui using the good starting guess as described in Table 2. The results for one selected case are shown in Figure 6, Figure 7 and Figure 8.

Table 4 Goodness of fit results for the optimum fits to an observed wave spectrum at Maui-A.

Observed Spectrum	Mean	Std	RMS error
True spectrum	0.008347	0.021977	
Optimum Fit	0.008345	0.020208	1.90e-006

For a given frequency, the direction distribution shows a much wider spectrum than the original data. This is also the reason why the energy at the peak is lower in the optimum fit than in the original. The energy content of the spectrum is conserved, and therefore when the fit return a wider spectrum at a certain frequency, the peak energy level decreases at this frequency.

The log spectra in Figure 8 show that the transition area between the wind-sea and swell component is not well captured by the fitting process. However, this might improve when fitting the log-spectrum instead of the normal spectrum, or putting a weighting on the low energy parts of the spectrum.

DISCUSSION & CONCLUSION

The test cases have shown that the peaks of the different components are well captured. However, the high frequency tails of the partition and the bimodality of the wind-sea spectrum is sometimes not well captured, especially when the

energy content is low. This is also observed for the measured spectra from Maui-A.
A possible improvement would be to give a weighting to the low energy content of the spectrum or to fit to the log-spectrum instead of the normal spectrum. In addition here, we have assumed fixed values for α_{3i} and α_{3i} for all components. By also fitting these terms, we would make our model form considerably more flexible.

Conversely, one should be aware of the limitations of the data. The measured wave spectra are usually obtained from 3-component directional wave buoys returning 3 orthogonal translations, which are then transformed into the first 4 components of a Fourier expansion. Therefore, the resolution of the directional distribution is limited. Similarly, hindcast models are likely to be limited to the accuracy of the physics in the model; e.g. discrete interaction approximation for the 3rd order resonance wave-wave interactions and numerical inaccuracies in the propagation of swell from the origin to the considered location.

Ultimately, the 2D fitting method can be used to feed back into the partitioning process, assisting in the identification of components and also their continuity through time.

ACKNOWLEDGMENTS

The authors would like to thank Shell, Todd Oil Services Ltd for the use of Maui wave data.

REFERENCES

[1] Ewans K.C., 1998, "Observations of the Directional Spectrum of Fetch Limited Waves", *Journal of Physical Oceanography*, Vol. 28, No 3., March 1998

[2] Ewans K.C., 2002, "Directional Spreading in Ocean Swell", *Proceedings of Ocean Wave Measurement and Analysis (2001)*, 2002

[3] Forristall G.Z and Ewans K.C., 1998, "Worldwide Measurements of Directional Wave Spreading", *Journal of Atmospheric and Oceanic Technology*, Vol. 15, April 1998

[4] Hanson, J. L and Phillips, O. M, 2001. Automated Analysis of Ocean Surface Directional Wave Spectra. *Journal of Atmospheric and Oceanic Technology*, **18**, 277-293.

[5] Hwang P.A., Wang D.W., Walsh E.J., Krabill W.B. and Swift R.N., 2000, "Airborne Measurements of the Wavenumber Spectra of Ocean Surface Waves. Part II: Directional Distribution", *Journal of Physical Oceanography,* Vol.30.

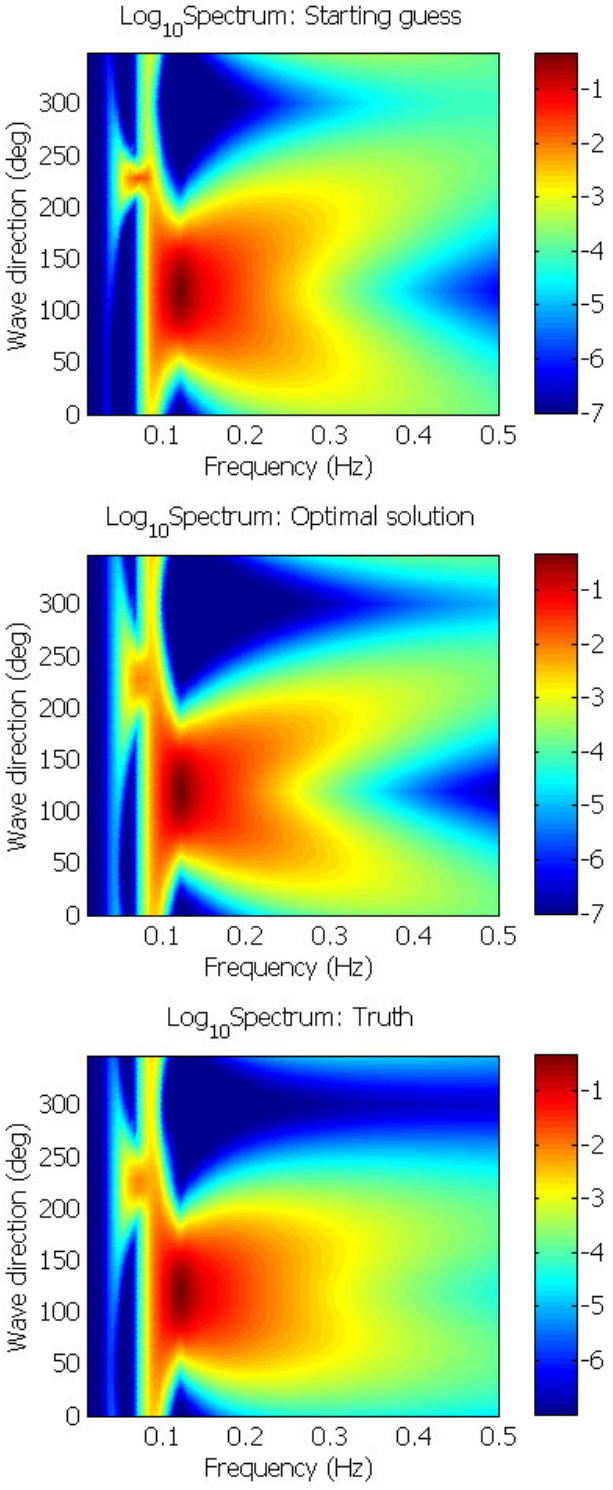

Figure 1 Log-spectra of case 1, pronounced wind-sea. Although the energy peaks is well fitted, the tail of the wind-sea partition is much wider in the optimal solution than in the true spectrum.

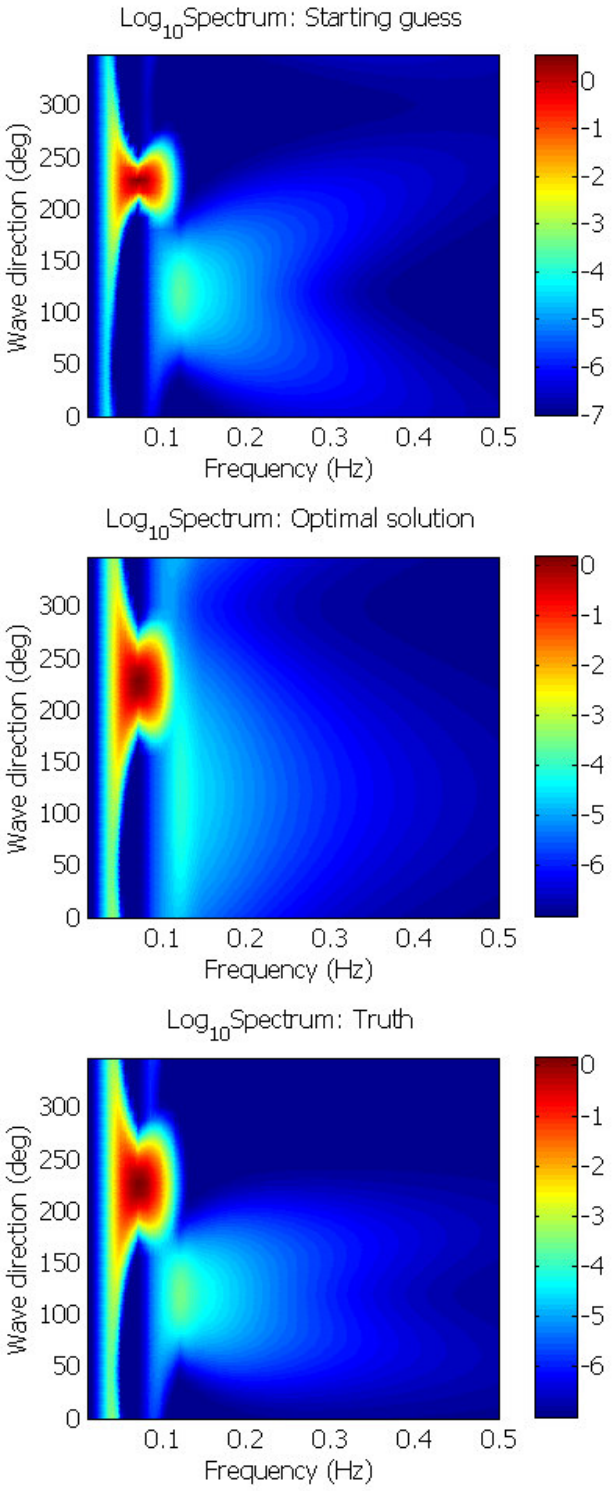

Figure 2 Log-spectra of case 2, pronounced swell partition. The width and energy peak of the swell is well fitted. The small wind-sea component is much more spread in the fit than in the true spectrum and the bimodality in the tail has not been properly captured.

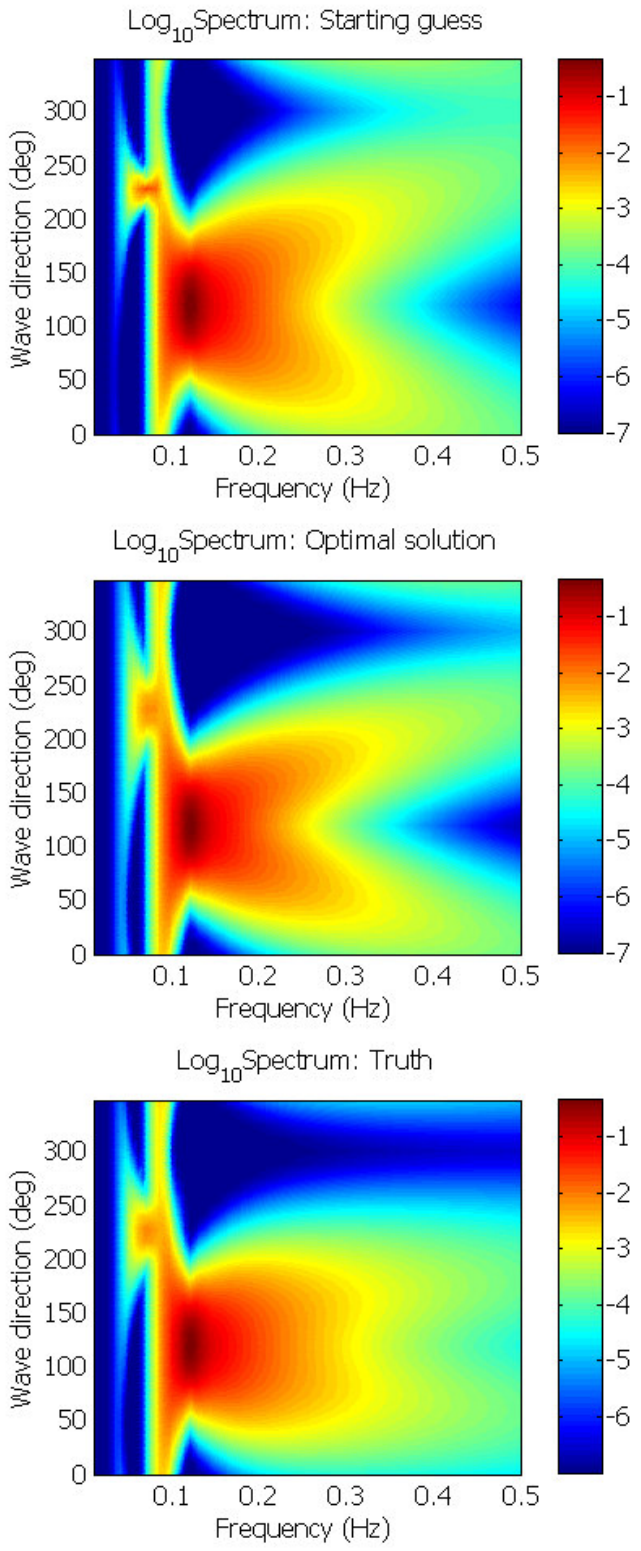

Figure 3 Log-spectra of case 3: pronounced sea and swell partition. For both spectra, the peak is well fitted, but again, the tail of the wind-sea is clearly much more spread than in the true spectrum.

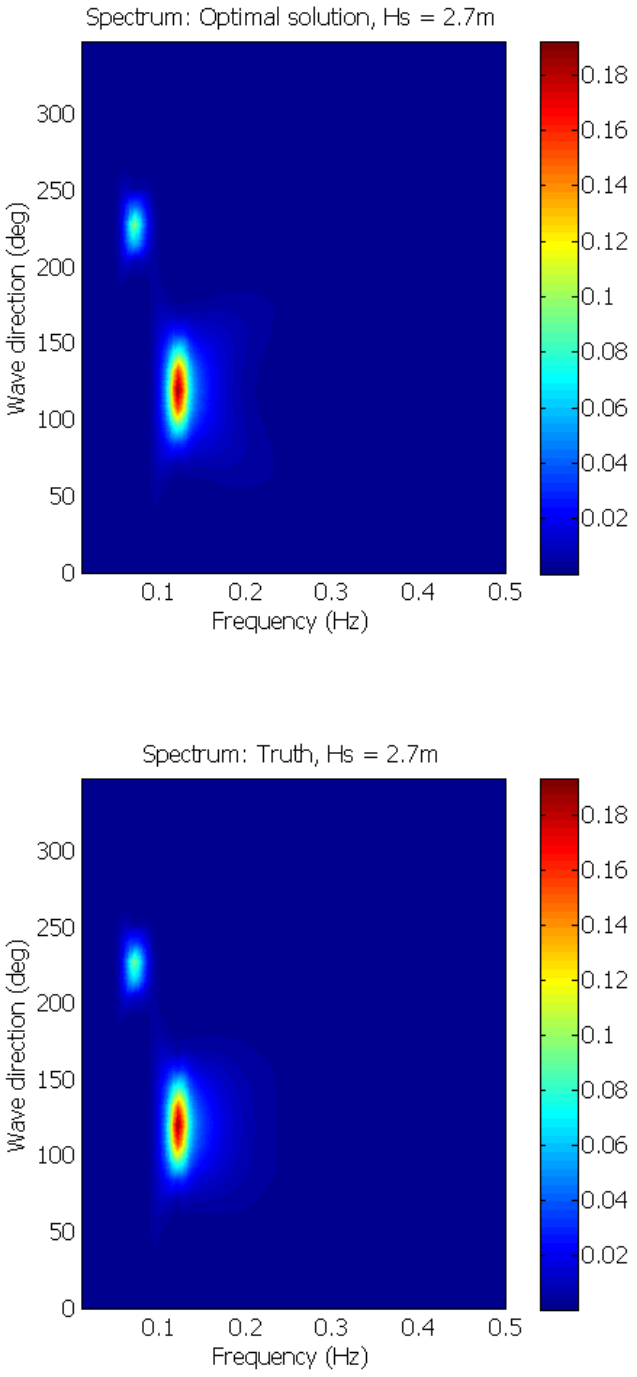

Figure 4 Spectrum for case 3: pronounced wind-sea and swell spectrum.

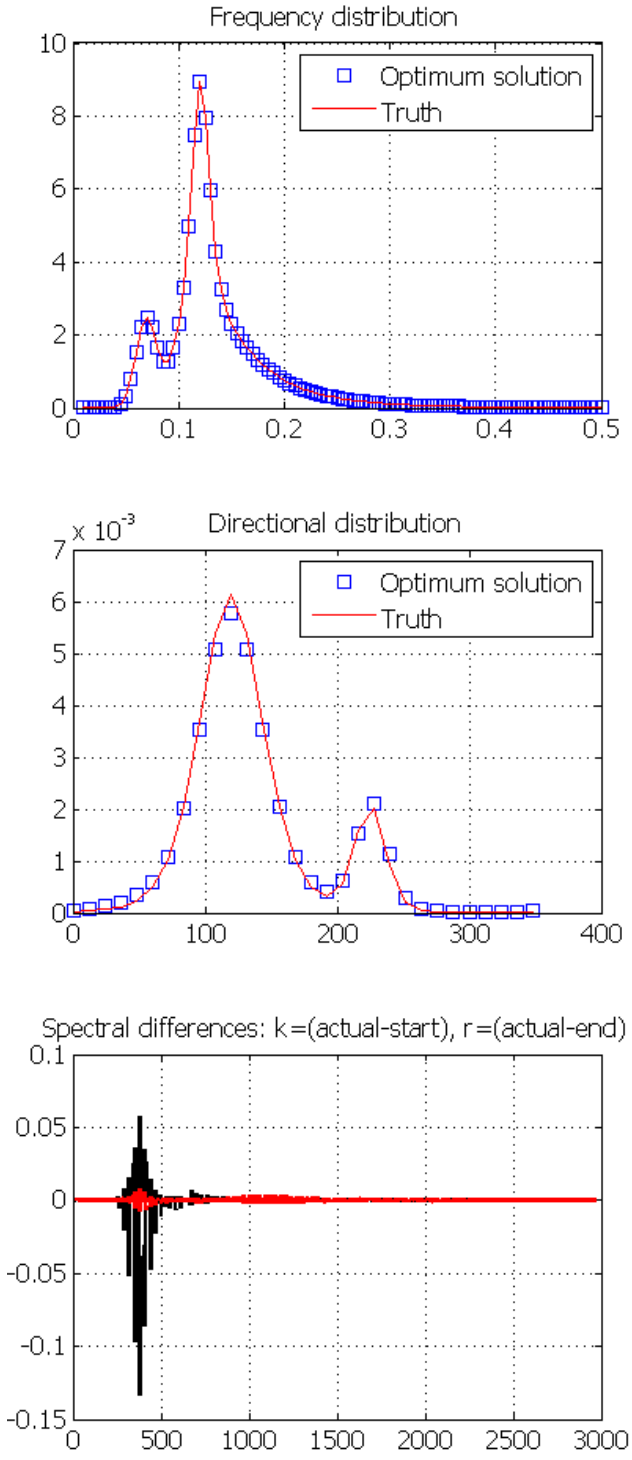

Figure 5 Frequency distribution and direction distribution for case 3. The lower plot gives the differences for each grid point (f_i, θ_j) of the input spectrum with the starting guess (black) and the optimum solution (red).

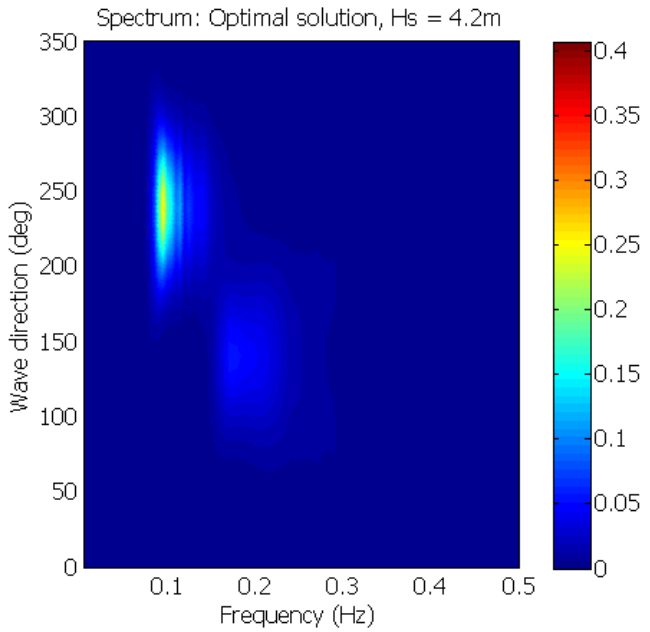

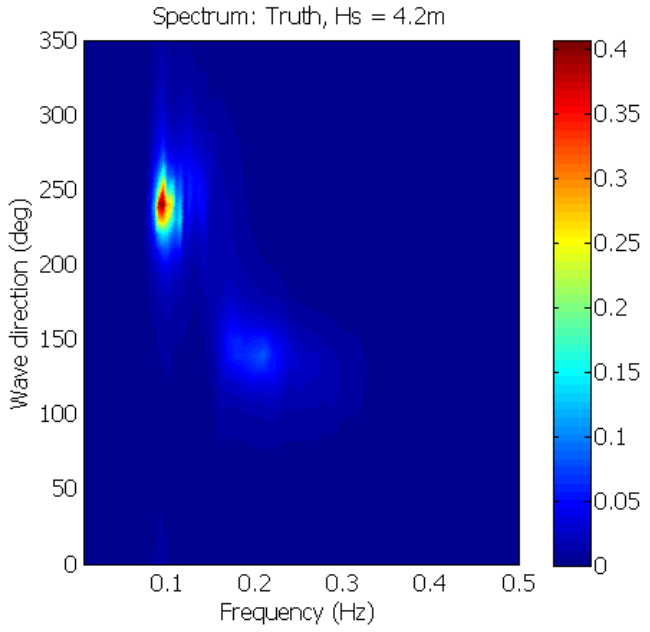

Figure 6 Optimum solution compared to a measured spectrum at Maui-A platform. The fit is much wider than the measurement at a given frequency, and therefore, the peak energy level at that frequency is lower.

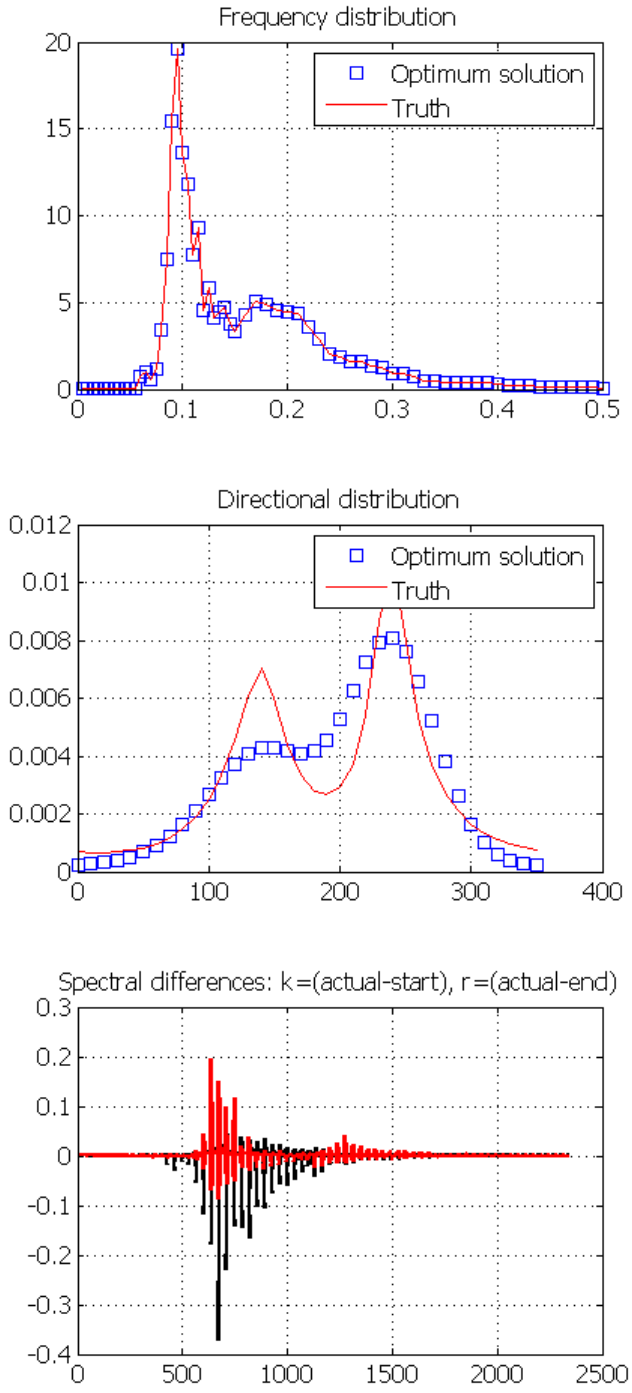

Figure 7 Optimum solution compared to the observed spectrum at Maui-A platform. The direction distribution captures the two peaks, but is less peaked than the measurement. The lower plot shows the spectral differences at each combination of frequency and direction $\left(f_i, \theta_j\right)$

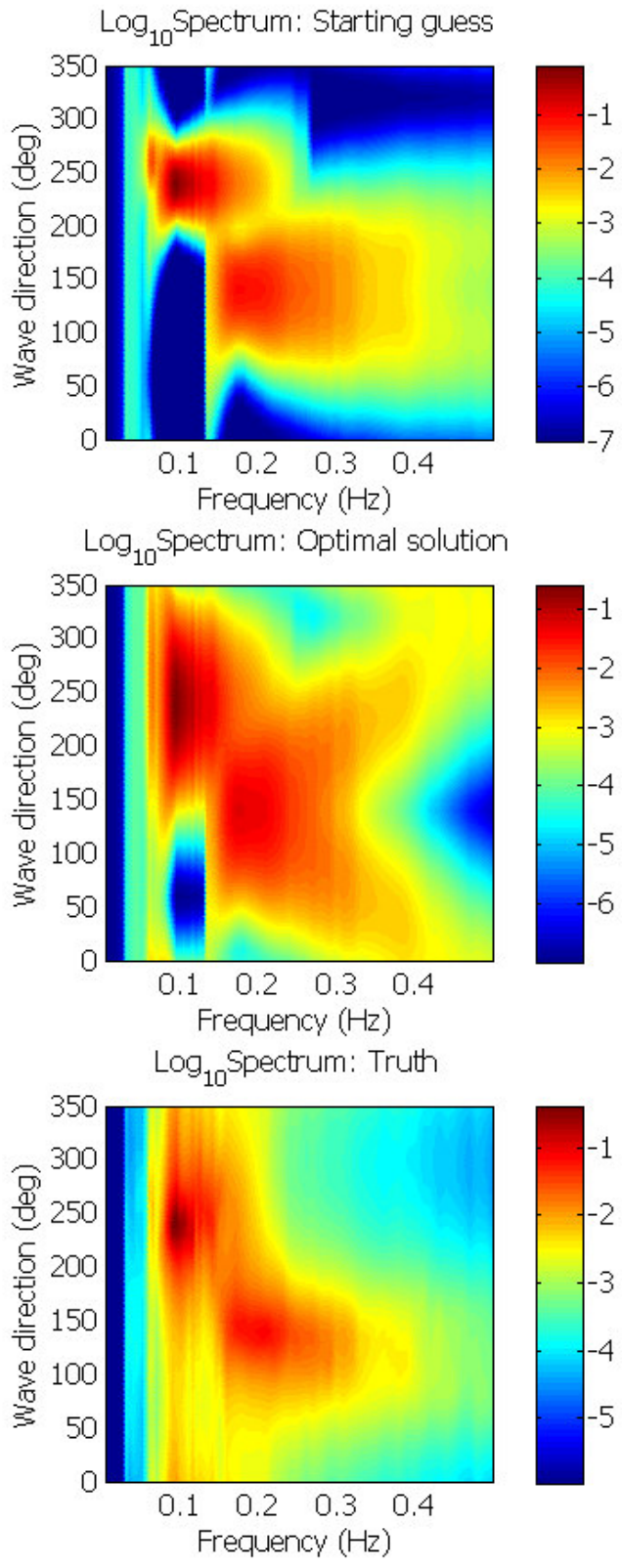

Figure 8 Log-spectra of a measured spectrum at Maui-A.